Integrating lateral swaying of pedestrians into simulations

Barbara Krausz and Christian Bauckhage

Fraunhofer IAIS, 53754 Sankt Augustin, Germany
{barbara.krausz, christian.bauckhage}@iais.fraunhofer.de

Abstract. Traditionally, pedestrian simulations are a standard tool in public space design, crowd management, and evacuation management. In particular, when minimizing evacuation times or identifiying hazardous locations, it is of vital importance that simulations are as accurate and realistic as possible. Although today's pedestrian simulation models give satisfying results in many cases, they are not realistic in highly crowded scenes. In this paper, we describe a characteristic motion pattern that is commonly observed in areas of high pedestrian density and that has not been taken into account in state-of-the-art pedestrian models. Hence, we extend an existing pedestrian model by integrating this characteristic motion pattern and show that our proposed model gives more realistic trajectories.

1 Introduction

Simulations of pedestrian streams play an important role when optimizing evacuation routes or idenfiying hazardous locations in a building or event location in order to prevent accidents. Considering future research directions that integrate real-time information into simulations in order to foresee hazardous situations, prevent accidents, and recommend evacuation strategies in real-time, accurate pedestrian models are even more important.

In order to improve and validate models of pedestrian behavior, insights into human motion characteristics are needed. In particular, the dynamics in locations of high pedestrian density are of great interest. A very characteristic human motion pattern is lateral swaying. From common observations, it is known that people do not move along a straight line, but instead tend to swing laterally. In [1], we have shown that the relationship between the velocity and the amplitude of lateral swaying is even a linear relationship. Recently, this characteristic motion pattern has been exploited in order to detect congested areas by analyzing short-term motions from video surveillance cameras [2, 3].

However, a comparison of simulated trajectories and real trajectories reveals that lateral swaying has not been adequately taken into account in state-of-the-art pedestrian models. In this work, we extend the generalized centrifugal force model [4, 5] by superimposing an oscillation force that mimics lateral swaying of pedestrians. In addition to introducing the oscillation force, we also adapt the ellipse modeling space requirements of pedestrians to a reasonable size.

2 Related Work

Despite of many modifications of the social force model presented by Helbing et al. [6, 7] that have been proposed over the years [5, 8, 9], the model still cannot reproduce realistic motion behavior in areas of high pedestrian densities. Overlapping of pedestrians can hardly be avoided making a higher repulsive force between pedestrians necessary. As a consequence, oscillations occur when high repulsive forces push pedestrians back and forth. In their *centrifugal force model*, Yu et al. [9] take the relative velocity of people into account and introduce a collision detection technique in order to avoid overlappings. However, by introducing a collision detection procedure, the centrifugal force model as proposed in [9] increases the complexity of the model and counteracts the idea of a force-based system. Thus, Chraibi and Seyfried [4,5] propose the *generalized centrifugal force model* (GCFM) in which they replace the collision detection technique in favor of an improved formulation of repulsive forces.

3 The Generalized Centrifugal Force Model

In the following, we briefly describe the *generalized centrifugal force model* and use the notation of Chraibi and Seyfried [5].

Given pedestrian i with coordinates $\overrightarrow{R}_i$ and mass m_i, the movement of i is described as the superposition of a driving force and repulsive forces:

$$m_i \ddot{\overrightarrow{R}}_i = \overrightarrow{F_i^{drv}} + \sum_{j \in \mathcal{N}_i} \overrightarrow{F_{ij}^{rep}} + \sum_{w \in \mathcal{W}_i} \overrightarrow{F_{iw}^{rep}}. \tag{1}$$

The *driving force* models motion into the direction of the pedestrian's intended destination as well as his desired speed v_i^0. Formally, the driving force of pedestrian i is given as

$$\overrightarrow{F_i^{drv}} = m_i \frac{\overrightarrow{v_i^0} - \overrightarrow{v_i}}{\tau} \tag{2}$$

where $\overrightarrow{v_i}$ denotes i's current velocity and τ is a relaxation time.

Repulsive forces induced by nearby pedestrians as well as obstacles model the avoidance of collisions. In [5], the repulsive force between pedestrians i and j is given as

$$\overrightarrow{F_{ij}^{rep}} = -m_i k_{ij} \frac{(\eta_{ped} \|\overrightarrow{v_i^0}\| + v_{ij})^2}{dist_{ij}} \overrightarrow{e_{ij}}. \tag{3}$$

With $\overrightarrow{R_{ij}}$ being the vector pointing from pedestrian i to pedestrian j, $\overrightarrow{e_{ij}}$ is the normalized connecting vector:

$$\overrightarrow{R_{ij}} = \overrightarrow{R_j} - \overrightarrow{R_i}, \; \overrightarrow{e_{ij}} = \frac{\overrightarrow{R_{ij}}}{\|\overrightarrow{R_{ij}}\|} \tag{4}$$

In order to model the field of perception, the coefficient k_{ij} in Equation 3 is at its maximum when pedestrian j is in the motion direction of pedestrian i,

whereas it is zero when pedestrian j is out of sight, i.e. when the angle between $\overrightarrow{v_i}$ and pedestrian j is greater or equal to 90°:

$$k_{ij} = \begin{cases} (\overrightarrow{v_i} \cdot \overrightarrow{e_{ij}})/\|\overrightarrow{v_i}\|, & \text{if } \overrightarrow{v_i} \cdot \overrightarrow{e_{ij}} > 0 \wedge \|\overrightarrow{v_i}\| \neq 0 \\ 0, & \text{otherwise.} \end{cases} \tag{5}$$

In addition to the field of perception, the relative velocity between pedestrians is also taken into account. If pedestrians in front of pedestrian i are walking fast, i is not affected by them:

$$v_{ij} = \begin{cases} (\overrightarrow{v_i} - \overrightarrow{v_j}) \cdot \overrightarrow{e_{ij}}, & \text{if } (\overrightarrow{v_i} - \overrightarrow{v_j}) \cdot \overrightarrow{e_{ij}} > 0 \\ 0, & \text{otherwise.} \end{cases} \tag{6}$$

However, if v_{ij} is small, the repulsive force decreases leading to overlappings. Chraibi and Seyfried take the intended speed $\|\overrightarrow{v_i^0}\|$ into account, since pedestrians with a high desired speed require higher repulsive forces in order to prevent collisions. They introduce a parameter η_{ped} to control the influence of the desired speed. In their experiments, they find a value of $\eta_{ped} = 0.3$ in order to minimize both overlappings and oscillations.

Next, $dist_{ij}$ in Equation 3 denotes the distance between pedestrians i and j which are modeled as ellipses. $dist_{ij}$ is the distance of the ellipses along the vector $\overrightarrow{R_{ij}}$ connecting the ellipse centers.

Pedestrian i is modeled as an ellipse centered on $\overrightarrow{R}_i$ with semi-axis a_i being the semi-axis in the movement direction $\overrightarrow{v_i}$ and b_i the semi-axis orthogonal to a_i. a_i includes physical body extensions of pedestrian i as well as space requirements in movement direction which depends on the current speed:

$$a_i = a_{min} + \tau_a \|\overrightarrow{v_i}\| \tag{7}$$

where a_{min} and τ_a are two parameters to be set.

With b_i, Chraibi and Seyfried model space requirements into lateral direction due to lateral swaying. From observations of trajectories, they model b_i as:

$$b_i = b_{max} - (b_{max} - b_{min}) \frac{\|\overrightarrow{v_i}\|}{\|\overrightarrow{v_i^0}\|} \tag{8}$$

where b_{max} is the maximum amplitude of lateral swaying which decreases to a minimum of b_{min}.

Similar to the repulsive force between pedestrians, the repulsive force exerted by the wall w is given in [5] as:

$$\overrightarrow{F_{iw}^{rep}} = -m_i k_{iw} \frac{(\eta_{wall}\|\overrightarrow{v_i^0}\| + \|\overrightarrow{v_i^n}\|)^2}{dist_{iw}} \overrightarrow{e_{iw}} \tag{9}$$

where $\overrightarrow{v_i^n}$ is the normal component of i's velocity vector to the wall and η_{wall} is a parameter controlling the influence of the intended speed on the repulsive force similar to η_{ped} in Equation 3. $dist_{iw_j}$ is the distance between the nearest point on wall w and the nearest point on the ellipse of pedestrian i. $\overrightarrow{e_{iw}}$ and k_{iw} are defined analogously to Equations 4 and 5.

4 Integration of Characteristic Human Motion Patterns

In contrast to the original social force model, the generalized centrifugal force model shows good results even in areas of high pedestrian density. However, a comparison of simulated trajectories and real trajectories reveals that lateral swaying has not been adequately taken into account. In the generalized centrifugal force model, pedestrians are modeled as ellipses which include space requirements into lateral direction due to lateral swaying, but pedestrians do not actually perform lateral oscillations. Instead, they are walking along a straight line.

Since the observation of lateral swaying is a fundamental characteristic of human gait and crucial for the detection of congested areas, see [3], we introduce an *oscillation force*. Thus, the movement of a pedestrian i with mass m_i and position $\overrightarrow{R}_i$ is modeled as the superposition of a driving force, repulsive forces as well as the oscillation force:

$$m_i \ddot{\overrightarrow{R}}_i = \overrightarrow{F_i^{drv}} + \overrightarrow{F_i^{osc}} + \sum_{j \in \mathcal{N}_i} \overrightarrow{F_{ij}^{rep}} + \sum_{w \in \mathcal{W}_i} \overrightarrow{F_{iw}^{rep}}. \tag{10}$$

where $\overrightarrow{F_i^{drv}}$, $\overrightarrow{F_{ij}^{rep}}$ and $\overrightarrow{F_{iw}^{rep}}$ are defined as described above and $\overrightarrow{F_i^{osc}}$ is defined as:

$$\overrightarrow{F_i^{osc}} = -m_i (2\pi f(\overrightarrow{v_i}))^2 s(\overrightarrow{v_i}) \sin(2\pi f(\overrightarrow{v_i})t + \phi_0) \overrightarrow{n_i}. \tag{11}$$

Here, $\overrightarrow{n_i}$ is the unit vector normal to the moving direction $\overrightarrow{v_i}$ and ϕ_0 is the phase of oscillation. $f(\overrightarrow{v_i})$ and $s(\overrightarrow{v_i})$ are the frequency and amplitude of lateral swaying where we use the findings from [1]. In this work, we analyzed real trajectories obtained from video recordings of a large scale experiment conducted under laboratory conditions. Based on the trajectories, we found a linear relationship between the velocity and the amplitude of lateral swaying as well as between the velocity and the frequency:

$$f(\overrightarrow{v_i}) = 0.44 \|\overrightarrow{v_i}\| + 0.35 \tag{12}$$

and

$$s(\overrightarrow{v_i}) = -0.14 \|\overrightarrow{v_i}\| + 0.21. \tag{13}$$

In addition to the introduction of an oscillation force, we adapt the ellipse modeling space requirements of pedestrians. Similar to Chraibi and Seyfried, we model pedestrian i as an ellipse with semi-axes a_i and b_i (Figure 1) and take empirical studies of human body dimensions into account. Weidmann [10] reports a mean value of 0.23 m for the body depth with the 97.5 percentile at 0.27 m. Next, according to Weidmann, the step length can be computed as:

$$l(\overrightarrow{v_i}) = 0.235 + 0.302 \cdot \|\overrightarrow{v_i}\|. \tag{14}$$

First, we note that the first term in this equation is almost equal to the body depth of 0.23 m given above. The second term in Equation 14 models space

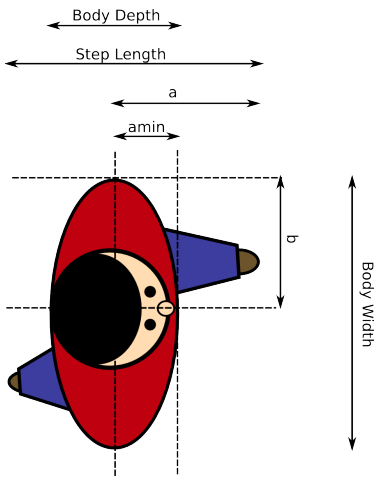

Fig. 1. A Pedestrian is modeled as an ellipse with semi-axis a_i being the semi-axis into the motion direction and b_i the orthogonal semi-axis. Note that b_i is half of the body width and a_i is half of the step length.

requirements of a pedestrian for taking a step. Having in mind that a_i denotes the length of the semi-axis and thus is half of the step length, we set it as follows:

$$a_i(\overrightarrow{v_i}) = 0.5 \cdot l(\overrightarrow{v_i}) = a_{min} + a_\tau \cdot \|\overrightarrow{v_i}\| \tag{15}$$

with $a_{min} \in \mathcal{N}(0.5 \cdot 0.23, 0.01) = \mathcal{N}(0.115, 0.01)$ modeling half of the body depth and $a_\tau \in \mathcal{N}(0.5 \cdot 0.302, 0.001) = \mathcal{N}(0.151, 0.001)$ modeling space requirements for taking a step.

The second semi-axis b_i is set to $b_i \in \mathcal{N}(0.5 \cdot 0.46, 0.01) = \mathcal{N}(0.23, 0.01)$, since Weidmann gives a value of 0.46 m for the body width with the 97.5 percentile at 0.5 m. Note that in contrast to the generalized centrifugal force model, we do not take lateral space requirements into consideration here, since they are already modeled by the oscillation force given in Equation 11.

5 Experiments

In order to evaluate the effectiveness of our model quantitatively, we simulate pedestrian movements and test if the fundamental diagram is well reproduced. Secondly, we employ trajectories obtained from an experiment of the Hermes project [11], use their initial positions and simulate pedestrian movements. A comparison of real trajectories to the simulated trajectories reveals that our model simulates realistic trajectories.

In our experiments, we use the parameters shown in Table 1.

For verification of the model proposed in Section 4 and to examine the influence of the two modifications (oscillation force and adaptation of ellipse), we

Parameter	Description	Value
r_c	cutoff radius	2
v_i^0	desired speed	$\mathcal{N}(1.34, 0.26)$
m_i	mass	1
τ	relaxation time	$\mathcal{N}(0.5, 0.001)$
η_{ped}	controls influence of intended speed on repulsive force	0.3
η_{wall}	controls influence of intended speed on repulsive force	0.2
δt	step size for solving differential equation system	0.001
GCFM [5]		
a_{min}	minimum length of semi-axis	$\mathcal{N}(0.2, 0.01)$
τ_a	factor for computing length of semi-axis	$\mathcal{N}(0.53, 0.001)$
b_{max}	maximum length of semi-axis	$\mathcal{N}(0.25, 0.001)$
b_{min}	minimum length of semi-axis	$\mathcal{N}(0.2, 0.001)$
modified GCFM (Section 4)		
a_{min}	minimum length of semi-axis	$\mathcal{N}(0.115, 0.01)$
a_τ	factor for computing length of semi-axis	$\mathcal{N}(0.151, 0.001)$
b_i	length of semi-axis	$\mathcal{N}(0.23, 0.01)$

Table 1. Parameter values used in the experiments.

simulate pedestrian trajectories in a corridor (26m × 1m) and measure the fundamental diagram in a measurement area (2m × 1m) located in the middle of the corridor.

In Figure 2, we depict resulting fundamental diagrams in comparison to experimental data [8]. Figure 2(a) shows the fundamental diagram for the original GCFM. In Figure 2(b), we superimposed the oscillation force (Equation 11), whereas in Figure 2(c), we adapt the size of the ellipses of pedestrians. Figure 2(d) shows the final model as proposed in Section 4 with oscillation force and adapted ellipse size.

When superimposing the oscillation force, the speed decreases, since pedestrians require more space for lateral oscillation. In the second case, when we just decrease the size of the pedestrians to a reasonable size, the speed increases due to less space requirements. Finally, when incorporating both modifications, the fundamental diagram fits well to experimental data.

Next, we compare simulated trajectories with real trajectories obtained from the Hermes dataset. For that purpose, we consider 30 seconds of a video which corresponds to the time of highest pedestrian density. We use the initial positions and velocities of 62 pedestrians and simulate their trajectories using the original GCFM as well as the modified GCFM with oscillation force and adapted ellipse size. Figure 3 shows real trajectories (green) and simulated trajectories (red).

Here, it becomes obvious that using the original GCFM, pedestrians do not perform lateral swaying. However, when using the proposed modified version of the GCFM, lateral oscillations can be observed. Note that there are differences between real trajectories and simulated trajectories using the modified GCFM, since we do not know the phase of lateral oscillation. Instead, we assume that the phase ϕ_0 in Equation 11 is zero.

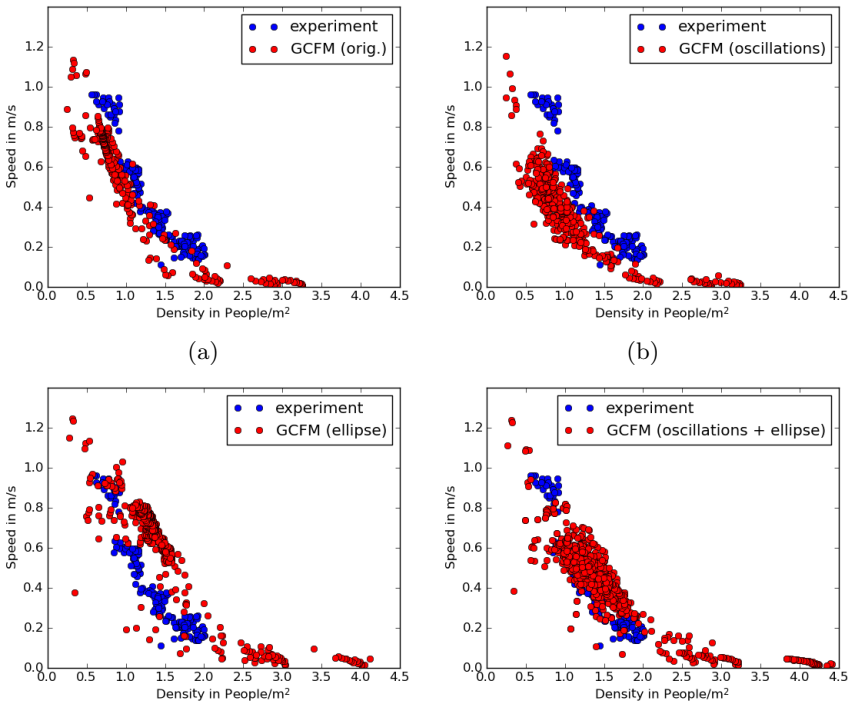

Fig. 2. Fundamental diagrams for comparing our proposed model and the original GCFM with regard to experimental data [8]. Pedestrian trajectories are simulated in a corridor (26m × 1m) using the (a) original GCFM, (b) superimposing the oscillation force, (c) adapting the ellipse sizes of pedestrians, and (d) using both modifications.

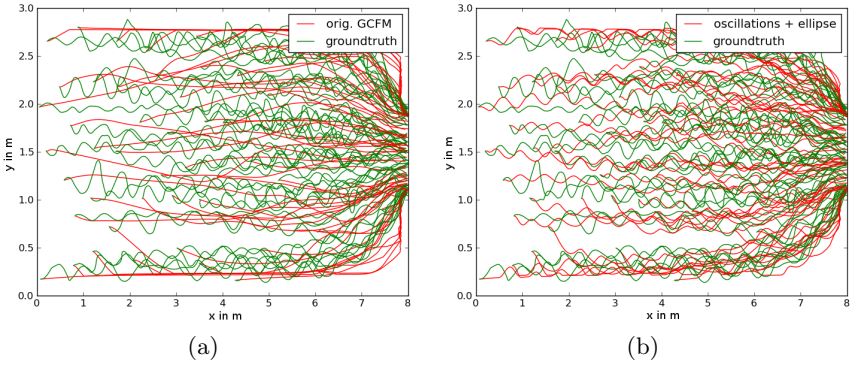

Fig. 3. Comparison of simulated trajectories to ground truth trajectories. In green, we depict the ground truth trajectories of 62 pedestrians. We depict the simulated trajectories in red for the (a) original generalized centrifugal force model [5] and (b) our proposed model. Note that we set the phase of lateral oscillation to zero.

		orig. GCFM	mod. GCFM
Hausdorff	Mean	0.29	0.26
	Standard Deviation	0.12	0.1
	Maximum	0.73	0.64
Length	Mean	120	87
	Standard Deviation	99	61.7
	Maximum	311	233

Table 2. Results of comparing real trajectories with simulated trajectories using the original GCFM and our modified version with oscillation force and adapted ellipse sizes. We compute mean, standard deviation and maximum of the Hausdorff distance as well as differences in trajectory lengths.

In order to compare simulated trajectories and real trajectories, we consider the differences in trajectory lengths as well as the Hausdorff distance. Table 2 shows mean, standard deviation and maximum of the Hausdorff distance as well as mean, standard deviation and maximum value of the differences in trajectory lengths. Obviously, the modified GCFM outperforms the original GCFM.

References

1. Krausz, B., Bauckhage, C.: Analyzing pedestrian behavior in crowds for automatic detection of congestions. In: ICCV-Workshop on Modeling, Simulation and Visual Analysis of Large Crowds. (2011)
2. Krausz, B., Bauckhage, C.: Automatic detection of dangerous motion behavior in human crowds. In: Advanced Video and Signal-Based Surveillance. (2011)
3. Krausz, B., Bauckhage, C.: Loveparade 2010: Automatic video analysis of a crowd disaster. Computer Vision and Image Understanding **116**(3) (2012) 307–319
4. Chraibi, M., Seyfried, A., Schadschneider, A., Mackens, W.: Quantitative description of pedestrian dynamics with a force-based model. In: Int. Conf. on Web Intelligence and Intelligent Agent Technologies. (2009)
5. Chraibi, M., Seyfried, A.: Generalized centrifugal-force model for pedestrian dynamics. Phys. Rev. E **82**(4) (2010) 046111
6. Helbing, D., Molnár, P.: Social force model for pedestrian dynamics. Physical Review E **51**(5) (1995) 4282–4286
7. Helbing, D., Farkas, I., Vicsek, T.: Simulating dynamical features of escape panic. Nature **407**(6803) (2000) 487–490
8. Seyfried, A., Steffen, B., Lippert, T.: The fundamental diagram of pedestrian movement revisited. Journal of Statistical Mechanics **P10002** 339–352
9. Yu, W.J., Chen, R., Dong, L.Y., Dai, S.Q.: Centrifugal force model for pedestrian dynamics. Phsical Review E **72**(2) (2005) 026112
10. Weidmann, U.: Transporttechnik der Fußgänger. Schriftenreihe des IVT 90, ETH Zürich (1992)
11. Hermes: BMBF Research Programme. `http://www2.fz-juelich.de/jsc/appliedmath/ped/projects/hermes` last visited April 26, 2012.